Research Paper

Assesment of Wound Dressing Properties of Medicinal Plants: The Case of *Hypericum perforatum* From Turkey

I. DEMIRHAN*

Vocational School of Health Services, Harran University, Sanlıurfa 63300, Turkey

Demirhan: Wound Dressing Properties of *Hypericum perforatum*

This study was aimed to investigate the performance of the extracted *Hypericum Perforatum* wound dressings produced by three different fabrication techniques. The effect of electrospinning, three dimensional printing, hydrogel casting techniques on the properties of the wound dressings were exhibited. Morphological, physical and chemical properties and differences of the resulting samples were established using Fourier transform infrared spectroscopy, scanning electron microscopy, mechanical and differential scanning calorimetry tests. Antimicrobial analysis of the patches was evaluated against *Escherichia coli* and *Staphylococcus aureus* strains. The results indicate that fabrication techniques affect the dressing patches utilizing surface chemical compositions and mechanical performances. Patches were highly effective against bacterial infections for both gram-negative and gram-positive. The highest area of the antibacterial effect belongs to the electro spinning case, which has 12 mm diameter on gram-positive bacteria thanks to the potassium rich surface chemistry of the fibers. In summary, these fascinating findings will lead to patches that can prevent over usage of antibiotics and the formation of new antibiotic resistivity. The plant *Hypericum perforatum* has the potential antibacterial effect for the *Escherichia coli* and *Staphylococcus aureus* strains. However, it was carried out for the first time that it could be used as a wound dressing

Key words: Three dimensional printing, *Hypricum perforatum*, wound dressing, natural products

Wounds occur as a result of traumatic or surgical disruption of tissue integrity due to destruction and injury. The presence of microorganisms around the wound increases the wound healing time[1]. *Staphylococcus aureus* (*S. aureus*), is a member of the Micrococcaceae family of *Staphylococcus* genus, which enters the tissue with mucosal injury, infection and surgical interventions and shows pathogenic behavior[2]. It has been reported that Gram-positive *S. aureus* causes serious life-threatening infections such as skin and soft tissue infections, widespread skin rash infections, sepsis and endocarditis, and organ infections with many virulence factors[3]. Although strong antibiotics are also used against microorganisms during the wound healing process, it causes the development of infections and mortality rates vary between 18 % and 61 %[4]. In this regard, antibacterial wound dressings that can destroy these microorganisms around the wound and prevent the growth and development of these microorganisms. Today, widely known antibacterial agents; heavy metals such as silver, zinc, copper, mercury, titanium and their oxides, as well as chemicals such as triclosan and benzalkonium chloride. It is reported that the use of antibacterial wound dressings made of metal particles such as silver and zinc is exposed to tissue and organ damage in the body. Chemical products such as triclosan have also been shown to be harmful and even banned in some countries[5]. The reason of using plants in medical fields is stated as the therapeutic properties of various substances[6,7]. In addition, it is known that during the use and excretion of natural agents, could cause much less side effects than chemical and synthetic biocides. For this reason, herbal and natural modern approaches in wound treatment have come to the fore recently[8].

***Address for correspondence**
E-mail: ilterdemirhan@gmail.com

Accepted 06 February 2024
Revised 18 April 2023
Received 09 February 2022
Indian J Pharm Sci 2024;86(1):54-63

Hypericum perforatum (HP) belongs to the Hypericaceae family and is a plant native to Asia and Anatolia. *Hypericum* (Guttiferae) species grow naturally between 750-3200 m altitudes in Turkey and have been used in traditional medicine for a long time. Some studies have focused on the effect of extracts prepared from this plant species against certain viruses and bacteria, and drug applications[9,10]. Studies have indicated that raw plant extracts prepared from above-ground parts of HP have strong antibacterial effects[11]. Polymers are among the most commonly used materials in wound dressings[12]. Poly Vinyl Alcohol (PVA) is a water-soluble synthetic polymer and frequently used in drug delivery systems, wound dressings, including contact lenses, due to its biodegradability and non-toxicity[13]. In recent trends, polymers used as smart host substrates involve various drugs, additives, growth factors, and plant extracts with antibacterial and anti-inflammatory properties[14]. The wound area is supported and protected with various agents applied to the infected area.

Three Dimensional (3D) printing is an innovative technology that enables the printing of models containing desired features layer by layer with the help of computers. It is used in various application areas such as machinery, the construction industry, food, medicine, tissue engineering, and even cancer research[15]. This technology, which has dramatically improved more in the last 10 y, has a serious potential to obtain connective, epithelial artificially, muscle, and nerve tissues and also functional wound dressings[16]. Electrospinning (ES) is another popular method of producing fibers in different diameters from micrometer to nanometer from various biopolymers by creating an electric field between two electrodes. Fiber diameters, which are detrimental to the drug release performances, may vary according to many factors such as the flow of polymer solution, voltage, the distance of solution to the electric field[17]. Cells are more prone to attach, proliferate and grow on the high surface area fibrous meshes[18]. While the structure of the fibers does not allow any interactions, could lead to microbial infection, it facilitates wound healing by providing the necessary and sufficient oxygen interaction for wound healing[19]. Film dressings are usually preferred due to the ease of application to joints (knees, ankles and elbows) due to their flexible natures[20]. Films can reduce both the overproduction of wound exudate and the development and progression of infection in the wound bed[21]. In addition, these transparent films allow the wound bed to be easily which is useful for healing the patient due to the reduced frequency of regeneration of the dressings.

In this study, HP incorporated wound dressings obtained *via* three different fabrication methods. To the best of our knowledge, it is the first study investigated wound care skills of the HP. The morphological, physical and chemical properties of the resulting samples were established with Fourier-Transform Infrared (FTIR), Scanning Electron Microscope (SEM)/Energy Dispersive X-ray (EDX), X-Ray Diffraction (XRD), mechanical and calorimetric tests. In addition, the release kinetics of HP was determined using Ultraviolet (UV)-spectroscopy. All of the techniques were optimised based on the process parameters and precursor solutions.

MATERIALS AND METHODS

Materials:

HP plant was obtained from a local supplier in Kahramanmaras-Turkey region during the flowering period. This plant grown in Turkey, and its herbarium was created on 23.06.1960 by Hayrettin KAYACIK, the head of the Turkish Botany Institute. This plant from the Hypericaceae family is preserved in the forest botanical garden with herbarium number 452[22]. Plant samples were dried in dry air, powdered and stored in sealed containers. PVA (MW:89 000-98 000 g/mol) was obtained from SIGMA-ALDRICH. Dimethyl Sulfoxide (DMSO), Glutaraldehyde (25 % solution in water) were obtained from MERCK. Ethanol was obtained from ISOLAB.

Extraction of the HP plant:

Dried parts of the plant were extracted with 96 % ethanol, followed by the complete removal of chemicals at 50°. The extract was stored at 4° until the solutions were ready.

Fabrication of the patches with 3D printing, electrospinning device and Q-film method:

20 % (w/v) PVA dissolved in water at an elevated temperature of 90° for 1 h. After the dissolution of polymers and cooling of the PVA solution, HP and DMSO were added to the PVA solution

at 1:3, respectively, and the viscous blend was formed at room temperature. The pore-geometry and the structure of the dressings were designed using Solidworks 3D design software. The shape of the dressings was designed to be discs with 30 mm×30 mm×1 mm dimensions. Polymer solutions were loaded into 10 ml syringes and connected to the needles with an inner diameter of 0.5 mm. 3D slicing and printing parameters were: Infill density of 60 %, a total layer of 4, extrusion multiplier of 7. Electrospinning solution was prepared by dissolving PVA in water 10 % (w/v) at 90°. After the cooling, 3 ml of the HP and 3 ml DMSO were added to the PVA solution to end up 10P3D3Q. All solutions were mixed with a magnetic stirrer at room temperature. Polymer solutions were loaded into a 10 ml syringe and connected to the capillary tube. Voltage ranged from 18 to 30 Kv was applied. The critical voltage, electrode distance, and feed rates were checked during the electrospinning process. PVA was dissolved in distilled water at 90° to prepare 15 % (w/v) solutions. After the solution was cooled down to room temperature and 3 ml DMSO and 3 ml HP was added. After the solution was poured into petri dishes (diameter of 15 cm), and solvent evaporation was performed in an oven at 37° for 48 h.

Characterisation of the patches:

The viscosity, density, and surface tension of all solutions were performed to identify physical properties. The solution viscosity of the 3D printed dressing, electrospun patch and Q-film were measured using a digital viscometer (DV-E, Brookfield AMETEK, USA) at room temperature. The density of solutions was analyzed using DIN ISO 3507-Gay-Lussac, a standard 10 ml density bottle. The surface tension of the solutions was determined using a Sigma 703D, Attention, tensiometer (Germany). Each test was repeated 3 times, and all equipment was calibrated before experiments.

Fourier Transform Infrared Spectroscopy (FTIR):

FTIR analysis was performed with a Jasco FT/IR-4700 model machine to determine the functional groups of the dressings to examine the bond structures. The measurements were examined at room temperature (23°) in the transmission mode over the range 4000–400 cm^{-1} and averaged over 32 scans with 4 cm^{-1} resolution.

Dimension Shape and Morphology Measurements (SEM):

The morphological characterisation of the dressings was exhibited using a Scanning Electron Microscope (SEM, EVO LS 10, ZEISS). Before imaging, samples were sputter-coated with gold-palladium for 120 s using a Quorum SC7620 Mini Sputter Coater. The applied accelerating voltage was 10 kV. The average fiber diameter and distribution were measured using image software (Olympus Analysis, USA). The EDX analysis was conducted to determine the presence of various elements in all samples. Before the tests, each sample was sectioned into five rectangular-shaped samples, 4 cm in length and 1 cm in width. The thickness of each tensile test specimen was measured using a high-accuracy digital micrometer (Mitutoyo, USA). The tensile strength and strain of scaffolds, electrospun patches and films were performed using a tensile tester (Shimadzu, Japan) utilizing special running software. All samples were subjected to test the speed of 5 mm/min until the breaking point at room temperature (23°). The thermal properties such as melting Temperatures (Tm) and glass transition Temperatures (Tg) of the electrospun patches were examined by using a Differential Scanning Calorimeter (DSC) (Shimadzu, Japan). Temperature ranges were adjusted from 25° to 100° for all patches, and the heating rate was selected as 10°/min. Firstly, HP powder with different concentrations were prepared in PBS 5 different concentrations (0, 25, 0,5, 1, 1, 5 and 2 µg/ml) to construct a linear calibration curve. The analysis was performed to investigate the release kinetics of HP inside the active dressings. Samples were cut into rectangles with an average weight of 5 mg each and then immersed in 1 ml of PBS (pH 7.4 at 37°) for 24 h to evaluate the drug release kinetics. For all samples, at the scheduled times (30 min, 90 min, 210 min, 24 h), PBS was removed from each sample, and 1 ml of fresh PBS was added again to resume the release test. UV spectroscopy (Shimadzu UV-3600, Japan) was used for analysing the HP releasing profile. HP release behaviours of all of the samples were analysed according to the first-order model.

Antibacterial analysis:

Antibacterial activities against two pathogenic bacteria (Gram-positive and Gram-negative) were investigated by the agar disk diffusion method.

These two bacteria species were chosen as they cause infection in the wound and skin and show resistance to many antibiotics. In addition, *E.coli* was chosen as nearly 80 % of the wound-causing microorganisms. Overnight cultures of *E. Coli* MTBB 100309 and *S. aureus* MTBB 130203 in Mueller-Hinton broth (Sigma Aldrich, USA) were used to prepare bacterial suspensions with in the same broth and adjusted to 0.5 McFarland turbidity standard ($1\text{-}2\times10^8$) inoculated on Mueller-Hinton agar plates by using an automated plate inoculator (Retro c80, AB Biodisk, Sweden). Disks (5 mm in diameter) were cut from composite dressings and exposed to UV light (254 nm) for 1 h for sterilisation. Sterilised disks were placed on the surface of bacteria inoculated Mueller-Hinton agar plates. Ampicillin containing disks (2 µg and 10 µg) were used as control groups for both gram-positive and negative. Plates were incubated at 37° for 18 h. According to the European Committee on Antimicrobial Susceptibility Testing (EUCAST) criteria, growth inhibition zones around disks were measured and evaluated.

RESULT AND DISCUSSION

Solutions were prepared by adding different concentrations of DMSO into PVA. The plant extract ratio was determined by trial and error method and based on previous studies as listed (Table 1). The physical properties of all solutions, such as density, surface tension, and viscosity, are critical parameters affecting the used methods[23]. One of the essential steps in both electrospinning and 3D printing methods is to determine the appropriate viscosity. In a typical 3D printing process, when the viscosity is higher than the optimum printing condition, the printing cannot be achieved with the desired pore diameters and layers. Likewise, in an electrospinning method, viscous solutions cannot form nanofibers with the desired fineness. Precursor solutions of the current study, the viscosity value should be close to 53.4 m. Pa. s for the 3D printing process to take place. Values above this point are too viscous to be printed and below that point is hard to achieve a stable structure. For the ES technique, viscosities around 53.67 m Pa.s result in uniform fiber diameters (Table 2).

Considering the surface tension and the viscosity ratios, the surface tension for the 3D printing process should be 37.78 mN/m, and for the electrospun process, it should be 36.04 mN/m. The density of the solutions more definit. Tween 80 was used as a surfactant to achieve a proper surface tension in ES because PVA concentration was high enough, and clogging of the nozzle was another parameter to control during the fabrication of the patches.

TABLE 1: CONCENTRATION VALUES OF THE USED MATERIALS IN AQUEOUS SOLUTIONS

Fabrication type	Sample ID	P content (wt %)	D content (wt %)	H content (wt %)	T content (wt %)
ES	10P	10	0	0	0
	10P/3D/1Q	10	3	1	2
	*10P/3D/3Q	10	3	3	2
	10P/5D/1Q	10	5	1	2
3D printed	20P	20	0	0	0
	*20P/3D/1Q	20	3	1	0
	20P/3D/3Q	20	3	3	0
	20P/5D/1Q	20	5	1	0
Qfilm	15P	15	0	0	0
	15P/3D/1Q	15	3	1	0
	*15P/3D/3Q	15	3	3	0
	15P/5D/1Q	15	5	1	0

Note: P: PVA, D: DMSO, Q: HP, T80: Tween 80. The symbol "*" indicates the working solution concentrations for specific fabrication techniques

TABLE 2: PHYSICAL CHARACTERISATIONS OF THE SOLUTIONS

Used solution	Density (g/cm^3)	Surface tension (m N/m)	Viscosity (m Pa.s)
ES (10P/3D/3Q)	1091	36, 04	53, 67
3D (20P/3D/1Q)	1225	37, 78	53, 4
Q film (15P/3D/3Q)	1348	39, 82	54, 5

Note: Physical characterizations of the solutions used in the specific fabrication process showed

FTIR analysis was carried out to investigate the functional groups of all of the samples (fig. 1). PVA-DMSO related infrared spectra were observed in PVA-DMSO-HP extract. FTIR spectrum of PVA-DMSO reveals presence of few absorption lines at wave-numbers (cm^{-1}): 752, 848, 1352, 1500, 1598, 1647, 2145, 2235, 2341, 2367.7, 2529.4 and 2729.4. These lines show small deviations from the lines reported and corresponded to the PVA-DMSO complex[24]. In FTIR spectra, some of the lines observed were related to PVA (905, 1091, 1376, 1452 in cm^{-1}). Extremely broad (OH) absorption peaks became distinctly visible in the present case due to the shrinking of broadness. These changes can be attributed to the removal of liquidus part (DMS, water and DMSO) in general and, in particular, DMS[25]. The oxygen of DMSO, being an electron donor, is expected to participate as a hydrogen bond acceptor and form a hydrogen bond with PVA, leading to the formation of a stable PVA-DMSO[26]. FTIR peaks of HP, nitro compounds at 1536.15 cm^{-1} and aromatic compounds at 1609.23 cm^{-1}, and this result is consistent with the literatur[27]. The XRD pattern of pure PVA reveals prominent peaks 2θ, 9.58, 11.59, 19.97, and 23.10[28]. PVA-DMSO gel films show diffraction peaks at 19.70, and 22.95 overlapped on a broad hump extended from 15 to 30. These peaks represent reflections from (101) and (200), a monoclinic unit cell revealing a semicrystalline behaviour of PVA[29]. The XRD specific peak of the HP plant is around 25, as in (fig. 2), and effects of this group can be observed in any other HP containing groups.

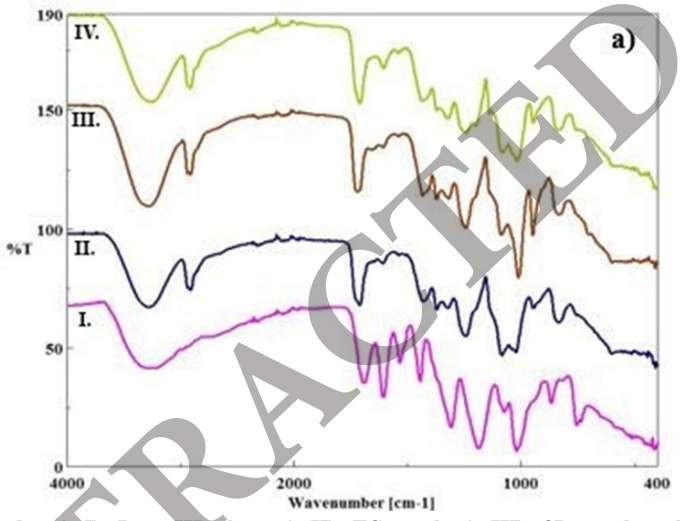

Fig. 1: FTIR spectra of the samples, (a-I): Pure HP plant; (a-II): ES patch; (a-III): 3D patch and (a- IV): Q-film; Q-film; X-ray diffraction patterns of samples

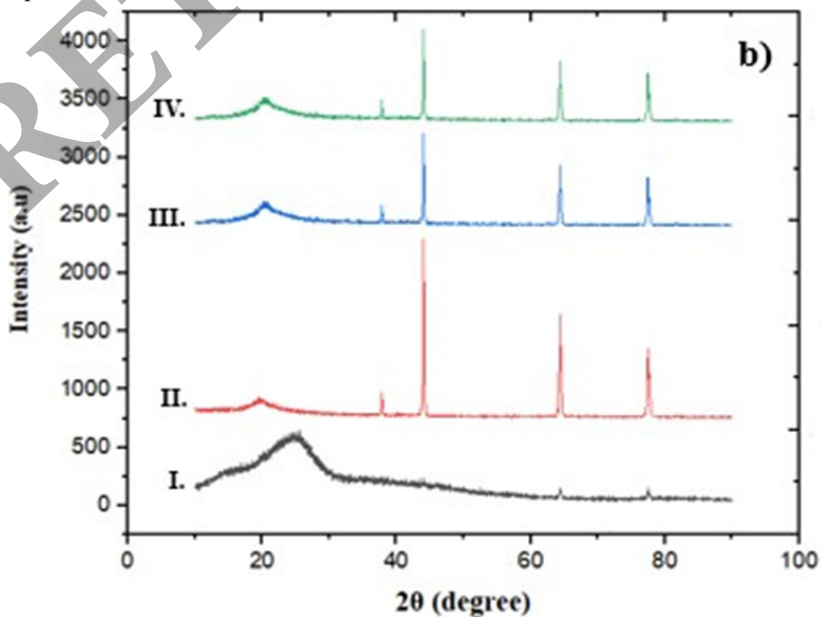

Fig. 2: X-ray diffraction patterns of samples, (b-I): pure HP; (b-II): ES patch; (b-III): 3D patch and (b-IV): Q-film

Scanning Electron Microscopy (SEM) was used to understand the morphology of the 3D printed patches, electrospun patches, and Q-film produced (fig. 3). Considering the EDX graphs (fig. 3a-fig. 3f), the Carbon (C) and Oxigen (O) elemental peaks of PVA coincide with the literature[30]. ES is a versatile technique to draw fibers from solutions of different polymers. An interesting result was found in EDX analysis of the nanofibers obtained *via* electrospinning. Potassium (K) peak can be observed in ES, while in 3D and film patches have no peak of potassium. This is apparently due to the content of the nanofibers in HP. Although the same amount of HP is inherent inside the other 3D patterned and film structures, there was no K peak that could be detected. This is firstly due to the electrical repulsion of the K ions during the flight of the nanofibers inside the PVA solutions. These K ions are accumulated on the surface of the fibers, because they are positively charged and given charge on them and also repel them through the outer surface of the nanofibers. In other techniques, K ions are distributed all over the structure, and therefore there is no peak present in EDX. The DSC thermogram (curved) indicates a strong endothermic transition around 308 K which shifts toward high temperature with an increase of polymer concentration. The occurrence of this endotherm is related to the interaction of DMSO with PVA. It has been shown that DMSO interacts with PVA and reduces Dimethyl Sulfide (DMS)[31]. PVA with a high degree of hydrolysis (98 %-99 %) usually melts in the temperature range where the thermal degradation of the polymer begins, and pure PVA has a melting peak between 200°-250°[32]. The DSC profile of the HP and the profiles of the samples prepared by three fabrication methods are as shown in (fig. 4). The mechanical properties of all samples were investigated at room temperature, as shown in (Table 3). Such results are crucial in determining the application area of the product. When we compare three methods among themselves, the highest strain failure was seen at Q-film and showed an elongation to approximately 88 % of its size. On the other hand, electrospun patches have shown much less strain at break than other methods because of the less water content[33]. However, the tensile strength of electrospun patches was higher than 3D printed ones but lower than Q-films. This is mainly due to the advanced water holding capacity of the films.

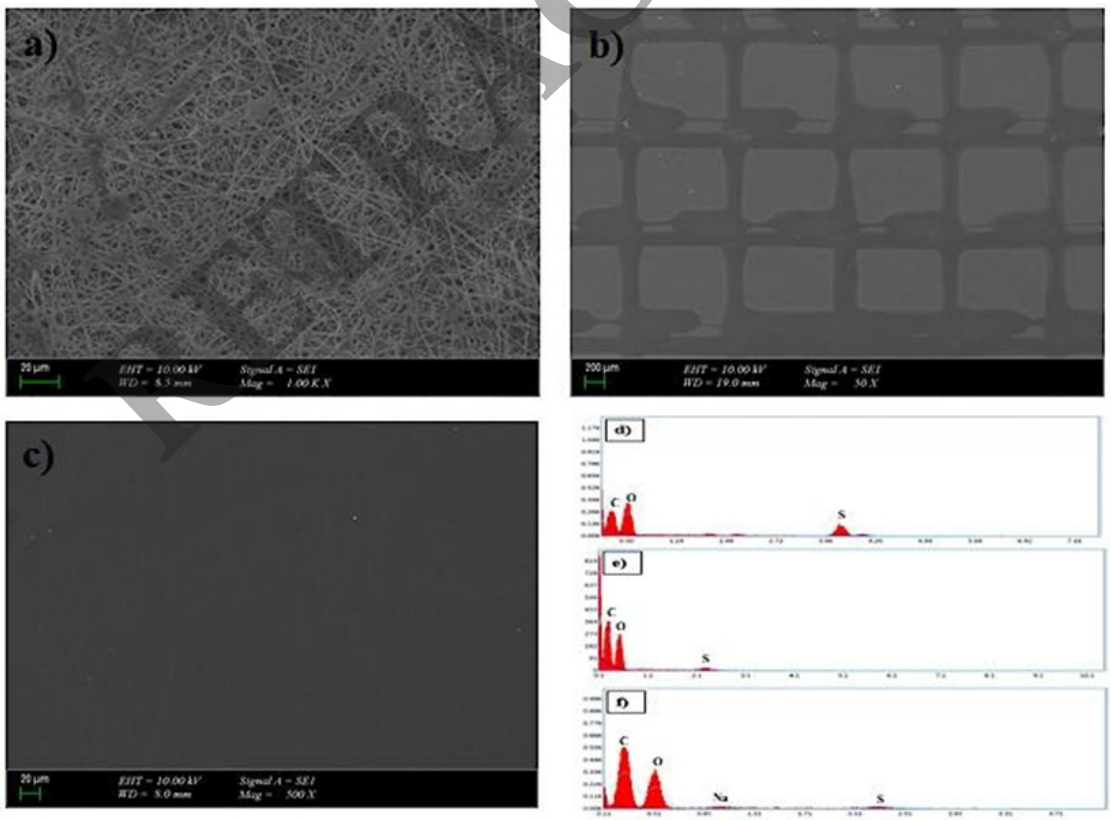

Fig. 3: Scanning electron microscopy images, (a): ES patch; (b): 3D patch; (c): Q-film, EDX results; (d): ES patch; (e): Q-film and (f): 3D patch

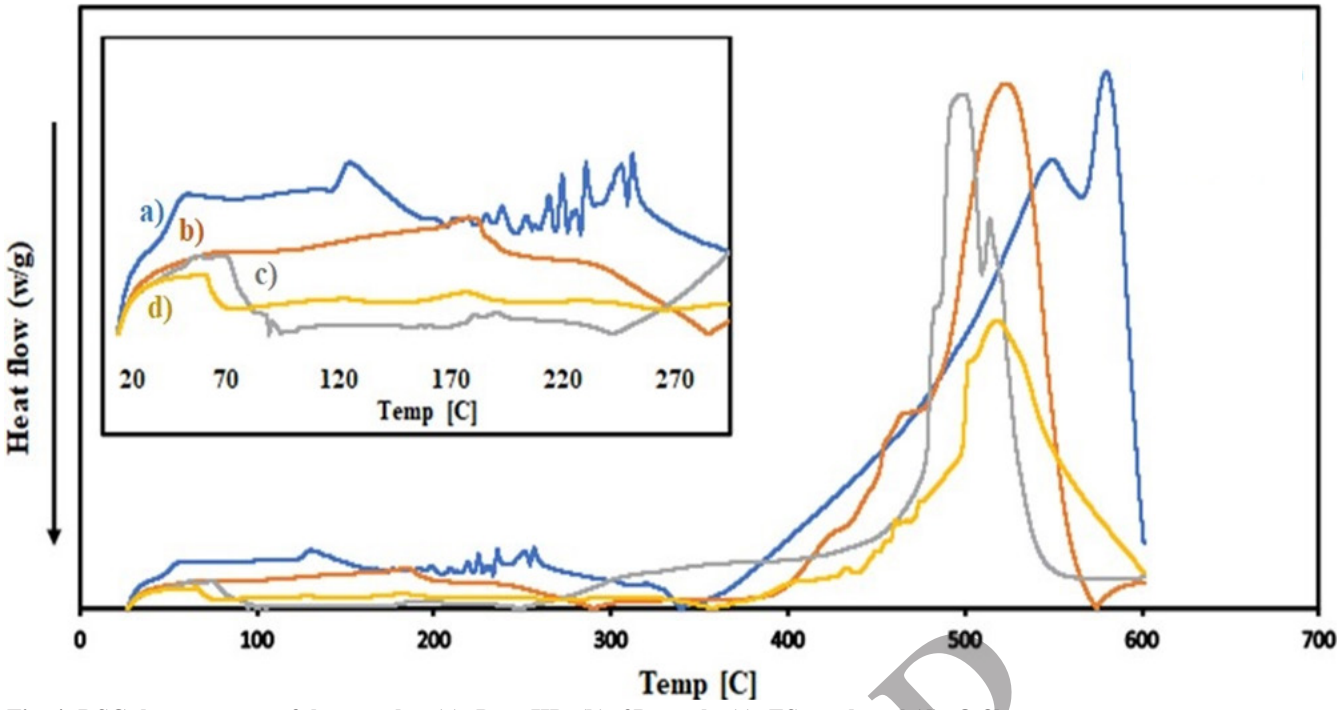

Fig. 4: DSC thermograms of the samples, (a): Pure HP; (b): 3D patch; (c): ES patch and (d): Q film
Note: ( ): *Hypericum perforatum*; ( ): 3D patch; ( ): ES patch and ( ): Qfilm

TABLE 3: TENSILE TESTING RESULTS OF ALL SAMPLES

Samples	Tensile strength (MPa)	Strain at break (%)
3D (20P/3D/1Q)	0.76±0.29	48.53±10.07
ES (10P/3D/3Q)	1.03±0.98	1.01±0.14
Q film (15P/3D/3Q)	3.81±1.51	88.68±57.97

Antibacterial activity of composite scaffolds was determined by disk diffusion assay, and the results were demonstrated in (fig. 5). Antibacterial activity of composites was examined with two bacterial strains, *S. aureus* and *E. coli*. While PVA/DMSO films have no antibacterial activity against the two bacteria, the HP plant effectively affects both of these two bacterial strains. This result was also consistent with our findings (fig. 6). Among the three methods, the highest effect has been demonstrated in Q-film. This is a versatile result as it can be applied to industries other than wound dressing like the food industry. The in vitro drug release kinetic assays for all samples produced by different methods of PVA-DMSO-HP extract were performed according to the first-order model. Firstly, a linear standard calibration curve was constructed with UV Spectra for HP extract. Absorption rates for HP (R^2=0, 9796) obtained for the quantitative determination of release (fig. 7). Then, 3D printed, electrospun patches and Q-film the release profiles of HP extract were measured in PBS and 37°, mimicking physiological conditions. Then, the cumulative emission rates are calculated according to the equation created with the calibration curve (fig. 7a and fig. 7b). The released HP absorbance value detected at 276 nm had almost a perfect fit. Moreover, cumulative release profile of HP (fig. 7c) in the first stage was very high. An intense release was seen in the first 30 minutes, with measuring ES patches 30.5 %, Q-film 23.9 %, and 3D patches 30.4 %.

In conclusion, we investigated the performance of the extracted HP wound dressings produced by three different fabrication (electrospinning, 3D printing, hydrogel casting) techniques. Instead of chemical and synthetic antibacterial agents that are known to have harmful effects on the environment and human health, completely natural and environmentally friendly herbal HP extracts together with PVA polymers, which are frequently used in the biomedical field, have been successfully produced by using electrospinning technique. Composite nanofibers, produced by combining the unique properties of nano-sized materials with completely natural and herbal solutions,

have revealed an innovative and environmentally friendly approach with potential use in wound dressing and wound treatment applications.

This study shows that the extract of the HP has the potential to be used in medical applications due to its antibacterial effect, this study will lead the further studies. HP's excellent antibacterial property and being a cross-linking material for the host PVA polymer makes HP a potential plant-based alternative to the overuse of antibiotics.

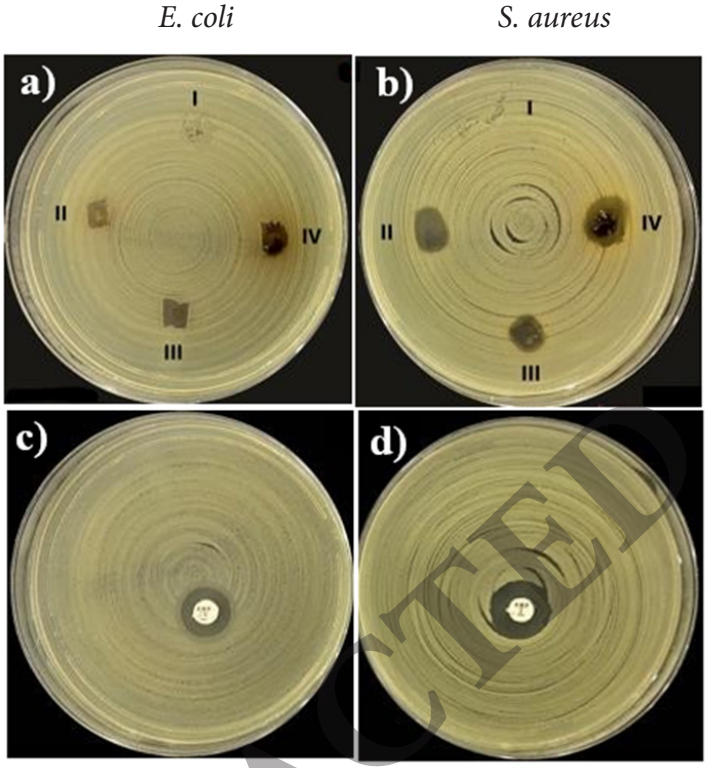

Fig. 5: Antibacterial effect of HP

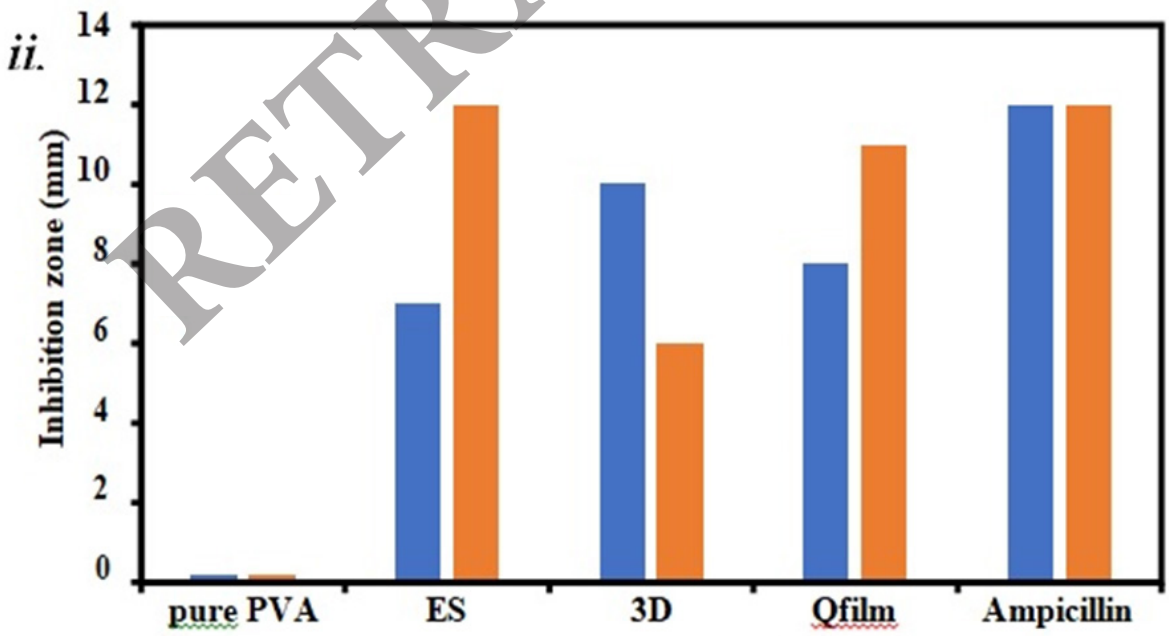

Fig. 6: The inhibition zones of composite scaffolds against, (a): E. coli (MTBB 100309) and (b): *S. aureus* (MTBB 130203) after 18 h incubation at 37°: (a-I): PVA- DMSO; (a-II): Electrospun patches; (a-III): 3D printed scaffold; (a-IV): Q-film; (b-I): PVA-DMSO; (b-II): Electrospun patches; (b-III): 3D printed scaffold; (b-IV): Q-film and (c): Control-AMP for E.coli and (d): Control-AMP for *S. aureus*
Note: (■): *E. coli* and (■): *S. aureus*

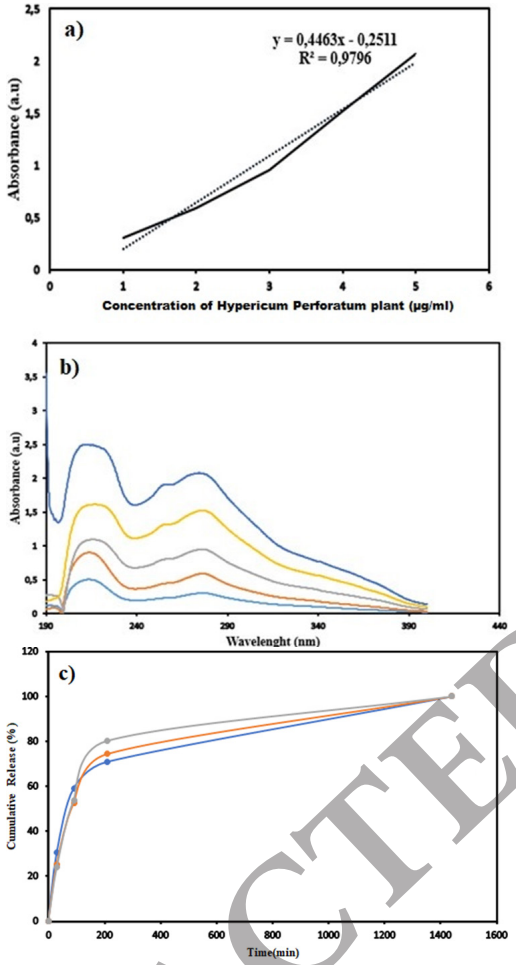

Fig. 7: *In vitro* HP release of samples, (a): HP Calibration curve; (b): Absorption spectra of HP at different concentration and (c) HP release profile

Note: (B): ( ): 0, 25 mg Q; ( ): 0, 5 mg Q; ( ): 1 mg Q; ( ): 1, 5 mg Q and ( ): 2 mg Q and (C): ( ): 3D patches; ( ): ES patches and ( ): Q-film

Acknowledgements:

This research is not supported any private institution.

Conflict of interests:

The authors declared no conflict of interests.

REFERENCES

1. Phaechamud T, Issarayungyuen P, Pichayakorn W. Gentamicin sulfate-loaded porous natural rubber films for wound dressing. Int J Biol Macromol 2016;85:634-44.
2. Namazi H, Rakhshaei R, Hamishehkar H, Kafil HS. Antibiotic loaded carboxymethylcellulose/MCM-41 nanocomposite hydrogel films as potential wound dressing. Int J Biol Macromol 2016;85:327-34.
3. Karatas E. Investigation of antibiotic resistance genes and the presence of panton-valentine leukoside in *Staphylococcus aureus* strains isolated from various clinical specimens. Gaziantep Univ Institute Health Sci Master Thesis 2015.
4. Ziemińska E, Strużyńska L. Zinc modulates nanosilver-induced toxicity in primary neuronal cultures. Neurotox Res 2016;29:325-43.
5. Gao Y, Cranston R. Recent advances in antimicrobial treatments of textiles. Textile Res J 2008;78(1):60-72.
6. Ozderin S, Fakir H, Donmez IE. Determination of essential oils and components of some thyme species naturally distributed in Mugla-Ula region, future of mediterranean forests: Sustainable society and environment, II. Natl Mediterranean Forest Env Symposium 2014.
7. Maver T, Maver U, Kleinschek KS, Smrke DM, Kreft S. A review of herbal medicines in wound healing. Int J Dermatol 2015;54(7):740-51.
8. Chopra R, Chopra I, Handa K, Kapur L. Indigenous drugs of India. 2nd ed. Calcutta India; 1958. p. 426.
9. Serkedjieva J, Manolova N, Zgórniak-Nowosielska I, Zawilińska B, Grzybek J. Antiviral activity of the infusion (SHS-174) from flowers of *Sambucus nigra* L., aerial parts of *Hypericum perforatum* L., and roots of *Saponaria officinalis* L. against influenza and herpes simplex viruses. Phytother Res 1990;4(3):97-100.
10. Tolkunova NN, Cheuva EN, Bidyuk AY. Effect of medicinal plant extracts on microorganism development. Pishchevaya Promyshlennost 2002;8:70-1.
11. Kırbag S. Antimicrobial effects of different extracts of *Hypericum perforatum* L. J Qafqaz Univ 1999;2:102-8.
12. Fundueanu G, Constantin M, Ascenzi P. Poly (vinyl alcohol)

microspheres with pH-and thermosensitive properties as temperature-controlled drug delivery. Acta Biomater 2010;6(10):3899-907.

13. Baker MI, Walsh SP, Schwartz Z, Boyan BD. A review of polyvinyl alcohol and its uses in cartilage and orthopedic applications. J Biomed Mater Res B Appl Biomater 2012;100(5):1451-7.
14. Toor A, Feng T, Russell TP. Self-assembly of nanomaterials at fluid interfaces. Eur Phys J E 2016;39:1-3.
15. Shi X, Zhou W, Ma D, Ma Q, Bridges D, Ma Y, *et al.* Electrospinning of nanofibers and their applications for energy devices. J Nanomater 2015;16(1):122.
16. Ozbolat IT, Peng W, Ozbolat V. Application areas of 3D bioprinting. Drug Discov Today 2016;21(8):1257-71.
17. Sikareepaisan P, Suksamrarn A, Supaphol P. Electrospun gelatin fiber mats containing an herbal—*Centella asiatica*—extract and release characteristic of asiaticoside. Nanotechnology 2007;19(1):015102.
18. Zamani M, Prabhakaran MP, Ramakrishna S. Advances in drug delivery *via* electrospun and electrosprayed nanomaterials. Int J Nanomed 2013;8:2997-3017.
19. Suwantong O. Biomedical applications of electrospun polycaprolactone fiber mats. Polym Adv Technol 2016;27(10):1264-73.
20. Wei L, Qin X. Nanofiber bundles and nanofiber yarn device and their mechanical properties: A review. Textile Res J 2016;86(17):1885-98.
21. Zuo W, Zhu M, Yang W, Yu H, Chen Y, Zhang Y. Experimental study on relationship between jet instability and formation of beaded fibers during electrospinning. Polym Eng Sci 2005;45(5):704-9.
22. Kayacık H. Orman Ve Park Ağaçlarinin Ozel Sistematiği Iii. Cilt Angiospermae. Istanbul Universitesi Orman Fakultesi 1975.
23. Thenmozhi S, Dharmaraj N, Kadirvelu K, Kim HY. Electrospun nanofibers: New generation materials for advanced applications. Mater Sci Eng B. 2017;217:36-48.
24. Pelipenko J, Kocbek P, Kristl J. Critical attributes of nanofibers: Preparation, drug loading, and tissue regeneration. Int J Pharm 2015;484(1-2):57-74.
25. Pillay V, Dott C, Choonara YE, Tyagi C, Tomar L, Kumar P, *et al.* A review of the effect of processing variables on the fabrication of electrospun nanofibers for drug delivery applications. J Nanomater 2013;8;128-42.
26. Lee KH, Kim HY, Bang HJ, Jung YH, Lee SG. The change of bead morphology formed on electrospun polystyrene fibers. Polymer 2003;44(14):4029-34.
27. Reneker DH, Yarin AL, Fong H, Koombhongse S. Bending instability of electrically charged liquid jets of polymer solutions in electrospinning. J Appl Phys 2000;87(9):4531-47.
28. Kaur S, Sundarrajan S, Rana D, Sridhar R, Gopal R, Matsuura T, *et al.* The characterization of electrospun nanofibrous liquid filtration membranes. J Mater Sci 2014;49:6143-59.
29. Li H, Williams GR, Wu J, Lv Y, Sun X, Wu H, *et al.* Thermosensitive nanofibers loaded with ciprofloxacin as antibacterial wound dressing materials. Int J Pharm 2017;517(1-2):135-47.
30. Kim JF, Kim JH, Lee YM, Drioli E. Thermally induced phase separation and electrospinning methods for emerging membrane applications: A review. Aich J 2016;62(2):461-90.
31. Laurencin CT, Nair LS. Nanotechnology and regenerative engineering: The scaffold. CRC Press; 2014. p. 233-9.
32. Arun M, Satish S, Anima P. Evaluation of wound healing, antioxidant and antimicrobial efficacy of *Jasminum auriculatum* Vahl. leaves. Avicenna J Phytomed 2016;6(3):295.
33. O'Meara S, Cullum N, Majid M, Sheldon T. Systematic reviews of wound care management: (3) antimicrobial agents for chronic wounds; (4) diabetic foot ulceration. Health Technol Assess 2000;4(21):1-237.